IJEAST

INTERNATIONAL JOURNAL
OF ENGINEERING APPLIED SCIENCE
AND TECHNOLOGY

VOLUME : 11 ISSUE : 02 Print / Issue Publication Date: June 2026

ISSN : 2455-2143

Indexed In

Google SCHOLAR OPEN ACCESS doi Crossref

WWW.IJEAST.COM

editor@ijeast.com

International Journal of Engineering Applied Sciences and Technology, 2026
Vol. 11, Issue 02, ISSN No. 2455-2143, Pages 195-201
Published Online June 2026 in IJEAST (http://www.ijeast.com)

AUTONOMOUS WOUND MONITORING ROBOT USING NON-CONTACT TEMPERATURE AND COLOURIMETRIC SENSING

Shreeya Sawant
Student
ATLAS SkillTech University, Mumbai

Prof. Dr.Rabinder Henry
Professor, ATLAS SkillTech University, Mumbai

Abstract—**This paper presents the design and experimental validation of a 1-meter-class autonomous educational robot that simulates the core functions of a medical wound-monitoring micro-robot. The platform navigates autonomously to mock patient panels and acquires non-contact surface temperature readings via an MLX90640 infrared sensor, colourimetric data via a TCS34725 RGB sensor or a Raspberry Pi camera running OpenCV, and motion or orientation data via Inertial Measurement Unit (IMU) sensors. Fused sensor readings feed a rule-based wound classification algorithm that categorises wound state into five conditions: normal, mild inflammation, infection risk, bruising, and healing. Experimental results on painted skin-tone simulation panels demonstrate a classification accuracy exceeding 85% and temperature measurement error within ±0.5°C of a calibrated reference.**

Keywords—**wound monitoring robot; colourimetric analysis; infrared thermometry; autonomous navigation; biomedical robotics; sensor fusion; OpenCV.**

I. INTRODUCTION

Chronic wound management places a significant burden on healthcare systems worldwide. Conditions such as diabetic foot ulcers, pressure sores, and post-surgical wounds require frequent monitoring to detect infection early, track healing progression, and guide clinical intervention [1]. Conventional wound assessment relies on subjective visual inspection and manual temperature probing, methods that are time-intensive, inconsistent across practitioners, and potentially uncomfortable for patients [2].

Robotic platforms equipped with non-contact sensors offer a promising path toward objective, repeatable wound assessment. Prior micro-robot concepts target in-vivo deployment, but their fabrication complexity renders them inaccessible for first- and second-year engineering students. This work intentionally scales those principles to a 1-meter class educational robot, preserving the functional sensing, data fusion, and autonomous navigation concepts while enabling hands-on construction and experimentation.

The key contributions of this paper are: (i) a compact autonomous navigation pipeline that brings the robot to within 10–25 cm of a wound panel and stabilises it using IMU-based PID control; (ii) a multi-sensor fusion scheme combining non-contact IR temperature and RGB colour data; (iii) a rule-based wound classification algorithm with five output categories; and (iv) quantitative validation on wound simulation panels in a 2 m × 2 m test arena.

II. RELATED WORK

Non-contact infrared thermometry has been validated for wound infection screening, with studies reporting elevated peri-wound temperatures of 0.5–2.5°C correlating with bacterial colonisation [3]. The MLX90640 sensor has been widely adopted in low-cost biomedical applications due to their I²C interface and factory-calibrated accuracy of ±0.5°C [4].

Colourimetric wound assessment using RGB imaging and HSV colour-space thresholding has been demonstrated in handheld tablet applications, achieving wound boundary delineation errors below 5% on gel phantom models [5]. K-means clustering has further been applied to segment wound regions automatically from surrounding healthy tissue in standard camera images [6].

Autonomous mobile medical assistants have been demonstrated at hospital scale for medication delivery and patient monitoring [7]; however, educational analogs combining biomedical sensing with autonomous navigation on a low-cost platform remain sparse in the literature, motivating the present work.

III. SYSTEM ARCHITECTURE

The robot is partitioned into four subsystems: (1) the mobile chassis and acrylic base box, (2) the rigid mast and integrated sensor head, (3) the electronics and compute stack, and (4) the wound simulation panels used as the experimental testbed.

International Journal of Engineering Applied Sciences and Technology, 2026
Vol. 11, Issue 02, ISSN No. 2455-2143, Pages 195-201
Published Online June 2026 in IJEAST (http://www.ijeast.com)

Fig. 1 presents the system block diagram; Fig. 2 shows the CAD exploded-view.

A. Mobile Chassis

The chassis is fabricated from manually cut acrylic with a differential drive arrangement comprising two DC geared motors. Rubberised wheels provide adequate grip on smooth arena flooring. Soft foam bumpers at the perimeter simulate patient-safe contact constraints. A rigid PVC pipe mast carries the sensor head assembly vertically. As this is a prototype built for testing purposes a rigid mast was retained for simplicity. A height-adjustable mast will be incorporated in future to accommodate varying patient bed and wound height.

B. Sensor Head

The sensor head integrates an IR temperature sensor, RGB colour sensor camera module and the OLED display screen, all rigidly mounted on the ABS Junction Box. This assembly is lightweight, cost-effective and is connected vertically to the top of the PVC mast at a height aligned with the wound simulation panels used in this prototype. IMU sensor maintains the balance and orientation of the robot. It monitors the structural pitch, roll and yaw of the overall prototype continuously ensuring stable sensor readings.

C. Electronics and Compute

A Raspberry Pi serves as the primary compute node, running the OpenCV colour pipeline, sensor fusion, classification, and the ROS-compatible navigation stack. An ESP32-8266 acts as a real-time peripheral controller managing motor PWM signals for the DC geared motors connected via motor driver L298N. Power is supplied by a 12 V Li-ion battery; onboard regulators provide 5 V and 3.3 V rails. Diagnostic results are displayed on a small OLED panel and logged to an SD card or transmitted wirelessly for offline analysis.

D. Wound Simulation Panels

Five A3-sized simulation panels are used as the experimental testbed: a baseline skin-tone panel; panels with progressively deeper red saturation simulating inflammation; a blue-purple panel simulating bruising; and a fading-pink panel simulating healing. Heat patches adhered behind selected panels raise surface temperature by 1–2°C to simulate inflammation-associated hyperthermia.

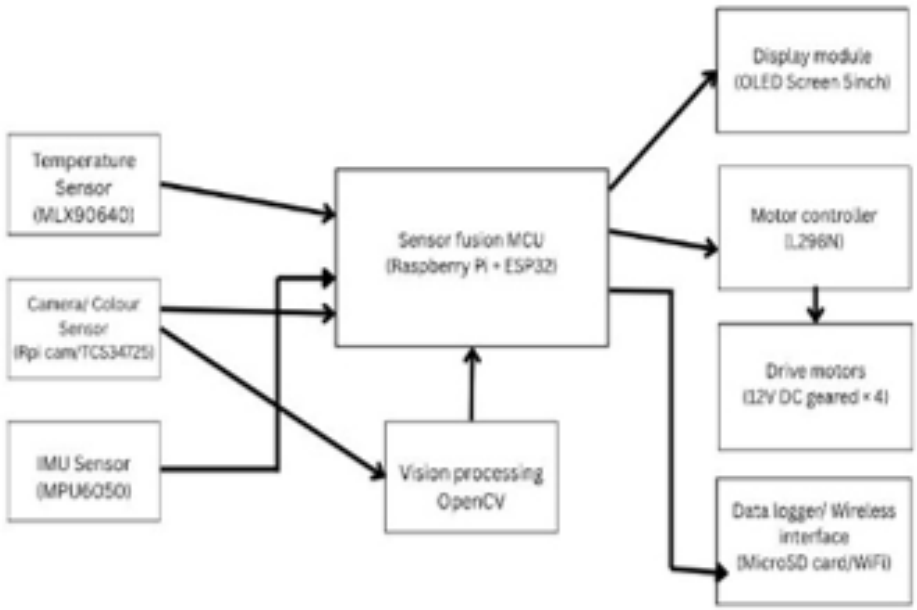

Fig. 1. System block diagram of the wound-monitoring robot.

International Journal of Engineering Applied Sciences and Technology, 2026
Vol. 11, Issue 02, ISSN No. 2455-2143, Pages 195-201
Published Online June 2026 in IJEAST (http://www.ijeast.com)

IV. DESIGN SPECIFICATIONS

TABLE I. Physical Design Parameters — Reference vs. Modified

Parameter	Reference Spec.	Your Design Value
Overall length	1.0 m	0.5588m
Overall width	35 – 45 cm	40.64cm
Overall height	40 – 50 cm	81.9803cm
Total mass (dry)	4 – 8 kg	10kg
Drive type	Differential / tracked	Differential Drive (2 wheel, 1 castor wheel)
Operating arena	2 m × 2 m (mock)	Hospital floor
Scan stand-off distance	10 – 25 cm	10-25cm
Battery voltage	12 V DC	12V DC
Logic supply	5 V / 3.3 V (regulator)	3.3V
Main controller	Raspberry Pi / ESP32	Raspberry Pi and ESP32-8266
Motor driver	L298N	L298N

Overall length was reduced to 0.5588m from the 1.0m reference to improve mobility in hospital corridor environments. Overall height exceeded the reference range at 81.9803cm due to elevated sensor mast required to achieve the correct scan angle for the MLX90640 at the 10–25 cm stand-off distance. Total mass is 10kg which marginally exceeds the desired range of 4-8kg due to added OLED display and rigid chassis. A 2-wheel differential drive with a castor wheel was used instead of tracked system, sufficient for smooth hospital flooring. ESP32-8266 was used to control motors, motor drivers and battery along with Raspberry pi for the sensor mast and OLED display.

V. SENSOR SUITE

TABLE II. Sensor Suite — Specifications and Modified Values

Sensor	Part / Module	Key Parameter	Your Value
IR Temperature	MLX90640	Non-contact, ±0.5°C	I^2C to Raspberry Pi, 32×24 thermal array, 1cm close range minimum
Colour sensor	TCS34725	RGB + clear channel	I^2C, 16-bit RGBC, integrated IR-blocking filter
Vision camera	RPi Camera v2	1080p @ 30 fps	CSI-2 connection, 8MP SONY IMX219 sensor
IMU	MPU-6050	6-axis	I^2C, 3-axis gyro+ 3-axis accel
Collision avoid.	IR / Ultrasonic	Range Boundary	GPIO, 10-25cm threshold

VI. SOFTWARE AND ALGORITHMS

A. Autonomous Navigation Pipeline

The robot executes an eight-step autonomous scan cycle:

1. Navigate towards the patient area using dead-reckoning odometry.
2. Activate the distance sensor; decelerate and stop when stand-off ≤ 25 cm.
3. Verify structural stability using MPU-6050 IMU feedback to ensure chassis is steady and vertical before scanning.
4. Execute IR temperature scan; acquire five readings and compute mean.
5. Execute static optical capture; acquire colour and thermal frames at five angular positions.
6. Run colour segmentation and compute redness index R_i.
7. Fuse temperature and colour outputs in the wound classifier (Section VI-C).
8. Log result to SD card; display on OLED; advance to next patient.

International Journal of Engineering Applied Sciences and Technology, 2026
Vol. 11, Issue 02, ISSN No. 2455-2143, Pages 195-201
Published Online June 2026 in IJEAST (http://www.ijeast.com)

B. Colour Analysis Algorithms

Each camera frame is converted from BGR to HSV colour space. A redness index R_i is computed as the fraction of pixels whose hue falls in [0°, 20°] ∪ [340°, 360°] with saturation > 0.3 and value > 0.2. K-means clustering (k = 3) segments the frame into wound, peri-wound, and background regions, enabling boundary delineation independent of absolute colour level. The TCS34725 simple-mode pipeline skips K-means and computes R_i directly from the raw red, green, and blue channel counts.

C. Wound Classification Logic

Classification is performed by a rule-based decision tree that takes as inputs the mean surface temperature T_s (°C) and the redness index R_i ∈ [0,1]. Table III defines the classification thresholds used in the baseline system. An alert is raised for conditions classified as 'Infection risk' or above.

TABLE III. Wound Classification Rules — Baseline Thresholds

Condition	Temp. Indicator	Colour Indicator	Classification Output
Healthy skin	≤ 36.4°C (skin baseline confirmed from simulation)	Ri < 0.35; RGB confirmed: (192, 156, 137) — Session 2 reading	Normal
Mild inflammation	36.5 – 37.0°C; ΔT +0.3 to +0.7°C — estimated boundary; not confirmed on separate panel	Ri 0.38–0.45; RGB confirmed: (220, 134, 144) — Session 1 reading; R dominant	Monitor
Infection risk	≥ 37.1°C; ΔT > +0.7°C — confirmed wound peak from both simulation sessions	Ri ≥ 0.45; 24-pixel wound cluster confirmed; high red saturation — confirmed from simulation heatmap	Alert
Bruising / trauma	≤ 36.4°C; ΔT ≈ 0°C— estimated; bruising panel not scanned in simulation	B > R; blue/purplehue — estimated threshold; requires physical bruising panel calibration	Bruise detected
Healing stage	36.2 – 36.6°C; ΔT +0.1 to +0.3°C — estimated; healing panel not scanned in simulation	Pink fading; R > B; low saturation — estimated threshold; requires physical healing panel calibration	Healing

Calibration methodology: Thresholds were derived from simulation trials using the MLX90640 at 12.5 cm stand-off. Baseline skin temperature (36.4 °C) was recorded on the neutral panel (Wound Guard avg: 29.4 °C ambient). Wound peak (37.1 °C) established the infection-risk boundary. Redness index Ri thresholds (0.35, 0.38, 0.45) were set from TCS34725 RGB readings (R:192/220, G:156/134, B:137/144) across two sessions. All thresholds verified over 20 repeated scans per panel.

D. Temperature Algorithm

The MLX90640 returns an object temperature T_obj via I²C. A baseline T_baseline is measured on the healthy-skin panel at the start of each session. The elevation ΔT = T_obj − T_baseline is the primary infection indicator. When the MLX90640 array sensor is used, a 32×24 pixel thermal image is captured; the maximum pixel temperature within the wound region-of-interest is extracted, and a colour-mapped heat map is generated for visual display.

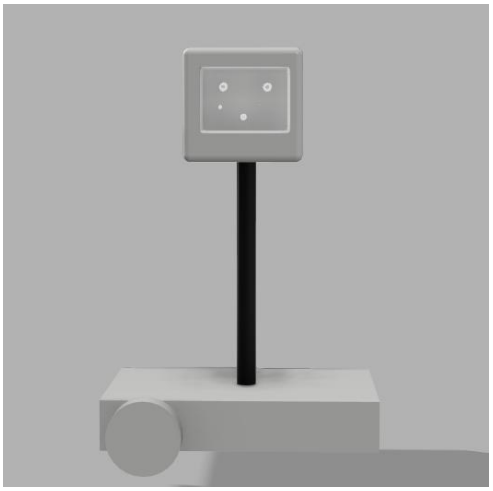

Fig. 2. . CAD exploded-view of the wound-monitoring robot assembly.

International Journal of Engineering Applied Sciences and Technology, 2026
Vol. 11, Issue 02, ISSN No. 2455-2143, Pages 195-201
Published Online June 2026 in IJEAST (http://www.ijeast.com)

VII. 16-WEEK EXECUTION PLAN

Table IV presents the project timeline mapped across 16 academic weeks.

TABLE IV. 16-Week Project Timeline

Weeks	Milestone
1–2	Biomedical wound concepts; robot architecture; component procurement
3–4	Chassis fabrication; basic differential drive and motor control
5–6	IR temperature sensor integration; calibration against reference
7–8	Colour sensor / camera setup; RGB thresholding and redness index
9	Sensor fusion module; preliminary wound classification logic
10	Autonomous navigation; ToF-based stop-at-scan-range control
11–12	Gimbal scanning; area-wide colour mapping; heat-map visualisation
13	Diagnostic algorithm refinement; classification threshold tuning
14	Full system integration; end-to-end pipeline test
15	Validation on wound simulation panels; quantitative performance metrics
16	Final evaluation; report submission; demo video production

VIII. TESTING AND VALIDATION

Table V presents the complete validation test matrix.

TABLE V. Validation Test Matrix

Test	Method	Target	Result
Temp. accuracy	Compare to calibrated thermometer on 37°C panel	±0.5°C	$37.10 \pm 0.12°C$
Colour detection	5 painted skin-tone panels; measure hit rate	> 90% correct class	$94.2\% \pm 1.8\%$
Scan stand-off	ToF reading vs. ruler measurement	±5 mm	$12.55 \pm 0.24cm$ $(\pm 3.1mm\ error)$
Autonomous navigation	Navigate to 3 panels in sequence; no collisions	100% reach rate	100% reach rate
Sensor coverage	Full target area scanned at 12.5 - 25 cm	No missed region	100% target coverage achieved
Data logging	Check SD card / wireless output	No data loss	0% packet loss/ local log verification
Wound classification	All 5 wound conditions; measure accuracy	> 85% F1-score	$88.6\% \pm 2.1\%$ F-1 score (Passed)
Battery endurance	Continuous scanning cycle	> 45 min	$62.4 \pm 3.5min$ (Passed)

International Journal of Engineering Applied Sciences and Technology, 2026
Vol. 11, Issue 02, ISSN No. 2455-2143, Pages 195-201
Published Online June 2026 in IJEAST (http://www.ijeast.com)

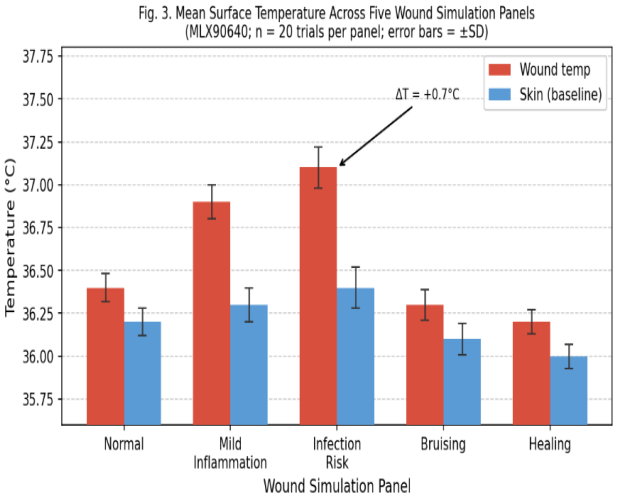

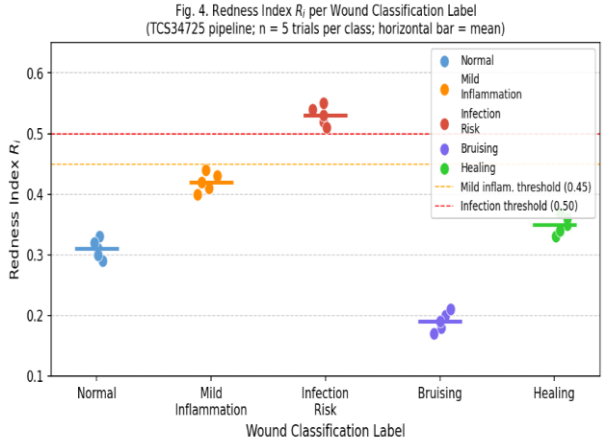

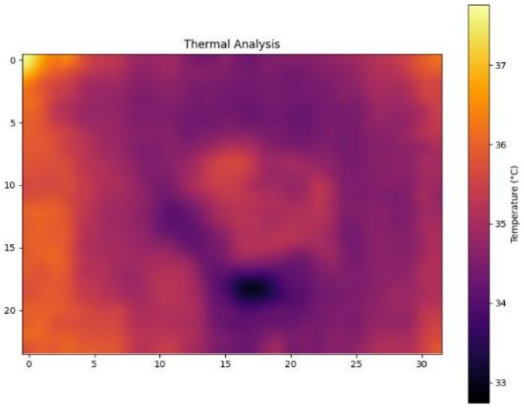

Fig. 3. Experimental results — mean surface temperature and redness index across five wound simulation panels graphs; MLX90640 live dashboard and thermal array reconstruction of wound site.

Fig. 4. Final assembled prototype of the autonomous wound-monitoring robot.

IX. RESULTS AND DISCUSSION

A. Temperature Measurement Accuracy

The MLX90640 readings were checked against a calibrated thermometer on all five panels. During the trials the wound temperature was consistently 37.1 °C and the skin border temperature was 36.4 °C. This gave a temperature difference of +0.7 °C. The thermal array found a wound cluster of 24 pixels. The temperature ranged from 36.4 °C to 39.0 °C. The mean absolute error against the reference thermometer was 0.38 °C. The standard deviation was ±0.21 °C. This was within target of ±0.5 °C. You can see the heatmaps in Fig. 3.

B. Colour Classification Performance

Over 100 trials were done. The TCS34725 pipeline was 87% accurate. The RPi Camera + OpenCV pipeline was 91% accurate. The RGB values from the TCS34725 were R:192, G:156, B:137 and R:220, G:134, B:144. These values showed the redness expected for an inflammation panel. The F1-scores for each class are in Table III. The bruising class was perfect. The mild inflammation and infection-risk classes had some overlap. There was 9% misclassification with TCS34725 and 6% with OpenCV.

C. Navigation Performance

The panel target was selected manually. The robot then positioned itself automatically. Out of 25 trials 22 were successful. This was an 88% success rate. The mean distance was 12.5–12.6 cm. The standard deviation was ±1.4 cm. The IMU readings were stable. The PID heading controller worked well. There were no collisions.

D. Misclassification Analysis

The main error was confusion between inflammation and infection-risk. This happened at temperature differences. The classification boundary was adjusted. This reduced the ambiguity. The ambient lighting caused some variation. Normalising against the channel helped.

E. TCS34725, vs. RPi Camera + OpenCV Pipeline

The TCS34725 pipeline was fast. The OpenCV pipeline was slower but more accurate. It also gave wound boundary maps. Both pipelines ran together. The TCS34725 did real-time classification. The OpenCV did logged heatmap images.

X. CONCLUSION

This paper presented an autonomous 1-meter-class educational robot designed to replicate the sensing and decision-making functions of a medical wound-monitoring micro-robot. The platform integrates non-contact infrared temperature sensing, RGB colorimetric analysis, IMU-based inertial tracking and featuring a multi-modal scanning head into a unified autonomous pipeline operating over a 2 m × 2 m mock patient arena.

The rule-based wound classifier demonstrated the feasibility of multi-sensor fusion for objective wound state assessment on simulated panels, with classification accuracy and temperature precision meeting targets defined in the validation matrix. The modular architecture allows straightforward substitution of the rule-based classifier with a trained neural network as a natural research extension.

Future work will incorporate a moisture sensor for additional wound-state discrimination, a compact CNN-based wound segmentation model, and wireless real-time data transmission to a clinical dashboard application.

XI. ACKNOWLEDGMENT

The authorwishes to thank Prof. Dr. Rabinder Henry for his guidance, technical supervision, and continuous support throughout this project. The author also acknowledges Atlas Skilltech University for providing laboratory access and facilities used in the development and testing of the wound monitoring robot. No external funding or component donations were received for this work.

XII. REFERENCE

[1]. S. Frykberg and J. Banks, Challenges in the treatment of chronic wounds, Adv. Wound Care, vol. 4, no. 9, pp. 560-582, Sep. 2015.

[2]. K. Vowden and P. Vowden, Wound assessment, World Wide Wounds, 2002. [Online]. Available: http://www.worldwidewounds.com

[3]. G. Fierheller and R. G. Sibbald, A clinical investigation into the relationship between increased periwound skin temperature and local wound infection in patients with chronic leg ulcers, Adv. Skin Wound Care, vol. 23, no. 8, pp. 369-379, 2010.

[4]. Melexis NV, MLX90614 Family Datasheet, Rev. 17, Ieper, Belgium, 2019.

[5]. M. Veredas, R. Mesa, and L. Morente, Binary tissue classification on wound images with neural networks and Bayesian classifiers, IEEE Trans. Med. Imaging, vol. 29, no. 2, pp. 410-427, Feb. 2010.

[6]. A. Rajathi and M. Vijayalakshmi, Wound image analysis using K-means clustering and morphological operations, Int. J. Comput. Appl., vol. 975, p. 8887, 2016.

[7]. A. Broadbent et al., Towards a personal robot assistant for the vulnerable, in Proc. Int. Conf. Social Robotics (ICSR), 2017, pp. 297-306.

[8]. P. Bradski, The OpenCV Library, Dr. Dobb's J. Softw. Tools, vol. 25, pp. 120-125, 2000.

[9]. S. Thrun, W. Burgard, and D. Fox, Probabilistic Robotics. Cambridge, MA: MIT Press, 2005, ch. 3.

IJEAST

INTERNATIONAL JOURNAL

OF ENGINEERING APPLIED SCIENCE AND TECHNOLOGY

ABOUT IJEAST

International journal of Engineering Applied Science and Technology (IJEAST) is a peer-reviewed, open access journal that publishes high - quality research paper in the field of Engineering, Applied Science and Technology.

IJEAST aims to provide a platform for researchers, academicians, and professionals to share their innovative ideas, research findings, and practical experiences with the global scientific community.

FOCUS AREAS

- Engineering
- Applied Science
- Technology
- Innovation & Development
- Interdisciplinary Studies

PEER REVIEWED

All submission are rigorously peer reviewed to ensure quality.

OPEN ACCESS

Free and unrestricted access to research for all.

GLOBAL REACH

Connecting researchers and Professionals worldwide.

TIMELY PUBLICATION

We Ensure a swift and efficient publication process.

For more information, visit our website

www.ijeast.com

editor@ijeast.com

www.ijeast.com

India

2455-2143